Experimental study of a subpicosecond pulse laser interacting with metallic and dielectric targets

L. M. Chen,[1,2] J. Zhang,[1,*] H. Teng,[1] Q. L. Dong,[1] Z. L. Chen,[1] T. J. Liang,[1] L. Z. Zhao,[1] and Z. Y. Wei[1]
[1]*Laboratory of Optical Physics, Institute of Physics, Chinese Academy of Sciences, Beijing 100080, China*
[2]*Laboratory for Laser Fusion, Institute of Nuclear Physics and Chemistry, Mianyang 621900, China*
(Received 14 August 2000; published 27 February 2001)

We have studied laser absorption, hot electron emission, and the energy spectrum of hot electrons produced during the interaction of a 150 fs, 5 mJ, 800 nm *p*-polarized laser pulse at $8\times10^{15}\,\mathrm{W/cm^2}$ with metallic and dielectric target materials. Because dielectric targets are much less conductive, the charge separation potential in dielectric targets is higher than that of metallic targets. This leads to a smaller laser absorption, fewer emitted electrons, and a lower hot electron temperature in dielectric than in metallic targets.

DOI: 10.1103/PhysRevE.63.036403 PACS number(s): 52.50.Jm, 52.40.−w, 52.25.Os, 52.38.−r

I. INTRODUCTION

The recent availability of intense ultrashort subpicosecond laser pulses [1] has enabled investigation of a new regime of laser-matter interaction in which intense laser pulses are deposited into a solid target faster than the target surface can hydrodynamically expand [2]. Thus, using high power laser systems of table-top size, it is now possible to study interaction physics under extreme conditions in relation to the fast ignition scheme for inertial confinement fusion [3], harmonic generation [4,5], and ultrashort x-ray generation [6], etc.

Previous measurements [7] of absorption of high contrast laser pulses have shown that at low laser intensities inverse bremsstrahlung (IB) is the main absorption mechanism and it is dependent on the electrical conductivity associated with an electron mean free path comparable to the interatomic spacing. However, at high intensities exceeding $3\times10^{15}\,\mathrm{W/cm^2}$, the absorption reaches ''resistivity saturation'' at a low level of 10% and becomes essentially independent of the target material. This behavior was attributed to the generation of a highly reflecting overdense plasma layer caused by rapid ionization of a thin front layer of the target. It seems that the plasma properties should be independent of the target material. However, Saemann and Eidmann [8] reported that the total x-ray emission from Al targets is much higher than that from glass targets with x-ray photons in the range of 1–20 keV. This implies that there are still many material dependent aspects in intense-laser–matter interactions. In particular, for laser pulses incident obliquely on targets, Brunel [9] and Gibbon and Bell [10] proposed that *p*-polarized laser pulses could be strongly absorbed by pulling electrons into vacuum during an optical cycle and then returning them to the surface with approximately the quiver velocity. This is called the ''vacuum heating'' (VH) mechanism [9].

In this paper, we report a systematic study of the laser absorption and hot electron emission from aluminum and glass targets (with a similar average *Z*) irradiated by intense ultrashort laser pulses with sufficiently high contrast such that the surface expansion is no greater than the peak amplitude of electron quiver motion during the interaction. We found that the total number of hot electrons with energies over 7 keV from aluminum targets was considerably more than that from glass targets. The charge separation potential we measured was greater than the prediction of Yang *et al.* [11,12], and in metallic targets this potential was found to be lower than that of dielectric targets because the free electrons partly ''neutralize'' the potential.

II. EXPERIMENTAL SETUP

The experiments were carried out at the Laboratory of Optical Physics of the Institute of Physics with a Ti:sapphire chirped pulse amplification (CPA) laser system operating at around 800 nm at a repetition rate of 10 Hz. The laser delivered 5 mJ energy in 150 fs pulses and produced a peak intensity on the target of $8\times10^{15}\,\mathrm{W/cm^2}$ at a laser focus of 20 μm diameter. The contrast ratio was approximately 10^{-5} at 1 ps before the peak of the pulse. The targets we used were 2 mm thick Al and glass plate targets. The roughness of the surface was less than 1 μm. The mount was controlled by microstep motors in the *xyz* dimensions to ensure that the laser interacted with fresh target surface at each shot.

The main diagnostic of fast electrons was a magnetic spectrometer, fitted with a permanent magnetic field of $B=380\,\mathrm{G}$. An array of LiF thermoluminescent dosimeter (TLDs) detectors was used behind the spectrometer to detect hot electrons. The recent development of ultrasensitive LiF TLDs provides the possibility of using thin TLDs for hot electron detection [13]. The energy range of this instrument covered from 7 to 500 keV. The collection angle of the spectrometer was on the order of 1×10^{-3} sr. Its energy resolution was better than 2%. Because the TLDs are insensitive to visible light, it was not necessary to use aluminum foils in front of the TLDs. The background of these TLDs was less than 1.2 μGy when they were heated to 240 °C.

The metallic target potential used to diagnose the total number of electrons emitted in each shot was measured directly by a fast oscilloscope (Tektronix TDS 520A) [14,15]. The leakage of the frequency doubled output of a *Q*-switched Nd:YAG (yttrium aluminum garnet) laser that pumped the CPA laser system was used to trigger the oscilloscope so as to ensure the synchronization of the detection signal with the femtosecond laser pulse. The target was connected by a very short wire to a sealed electric connector on one end flange of

*Author to whom correspondence should be addressed. Email address: jzhang@aphy.iphy.ac.cn

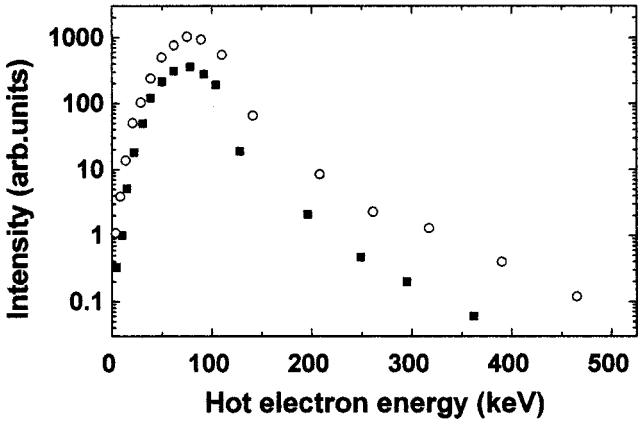

FIG. 1. The hot electron spectrum from Al (open circles) and glass (solid squares) targets irradiated by *p*-polarized femtosecond laser pulses at $8\times10^{15}\,\mathrm{W/cm^2}$.

the cylindrical vacuum chamber. Then the signal from the target was fed via a coaxial cable to the input of the oscilloscope. The input impedance of the oscilloscope of 50 Ω was matched to that of the connected cable in order to avoid reflection of signals. A Faraday cup 17 cm away from the target without a bias voltage in the direction normal to the target was also used to collect electrons emitted from the plasma.

The plasma absorption was measured by calorimeters. Slight focusing (with an $f/10$ lens) of the reflected beam ensured that all the scattering signals were collected by the calorimeters. An interference filter at a central wavelength of 800 nm was placed at the window of the calorimeter to ensure that only the reflected laser signal could be detected.

III. RESULTS AND DISCUSSION

All the experimental results presented here were obtained for laser pulses incident on targets at an angle of 45° with respect to the target normal without any prepulse.

The energy spectrum of the outgoing electrons was measured with the electron magnetic spectrometer shown in Fig. 1. The spectrum of ingoing electrons was measured indirectly by a NaI γ-ray spectrometer [16]. The hot electron spectrum resembles a bi-Maxwellian distribution. The low hot electron temperature is independent of target material and is generated by a resonance absorption mechanism with the scaling law $T_H\ (\mathrm{keV})\approx6\times10^{-5}(I\lambda^2)^{0.33}$ [17]. The high hot electron temperature is generated by the vacuum heating process [18,19]. This bi-Maxwellian hot electron distribution was also predicted by the simulation of Gibbon and Bell [10].

For the high hot electron temperature, the two diagnostics gave similar values. We can thus deduce that those outgoing and ingoing electrons are heated by the same mechanism [19]. The Al and glass targets were measured and the high hot electron temperature obtained for each: 62 keV for Al and 44 keV for glass targets. The number of hot electrons ($E_k>10\,\mathrm{keV}$) measured in this way for Al is almost four times greater than for SiO_2 targets.

The energy spectrum we measured is from the emission

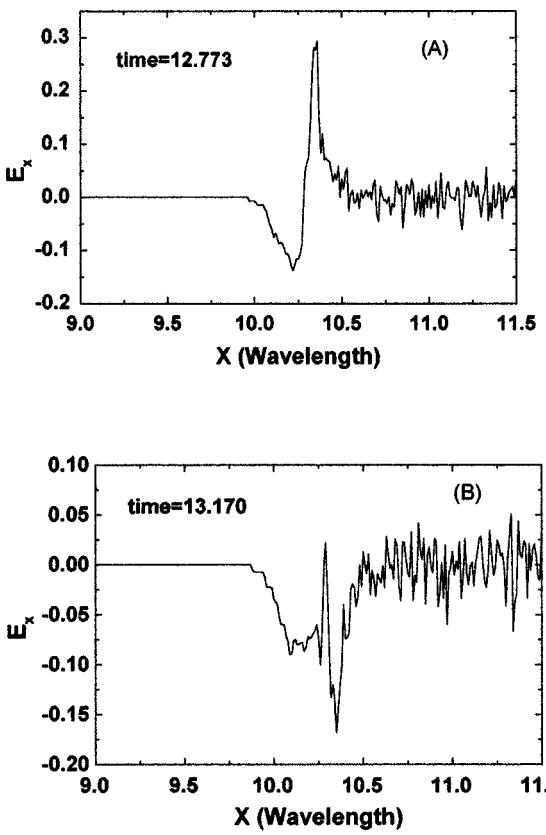

FIG. 2. The amplitude of the oscillating longitudinal electric field in Al targets at $t=12.773$ and 13.179 optical cycles of the laser field. The solid surface is at $X=10.3$ (>10.3 is into the target). The electric field at the target boundary changes its polarity periodically. The electric field here is in normalized units of $m\omega_0c/e$.

of hot electrons with energies greater than the charge separation potential (CSP) generated by less mobile ions. Those electrons with energies less than the CSP would be pulled back to the surface by the CSP. Figure 2 shows the normalized amplitude (in units of $m\omega_0c/e$) of the oscillating electric field in the direction normal to the solid surface. Here m is the mass of an electron, ω_0 is the laser frequency, c is the speed of light and e is the charge of an electron. The $+x$ direction in Fig. 2 is in toward the target. The simulations used a one-dimensional 1D fully electromagnetic LPIC++ code, where an electromagnetic wave is launched obliquely from the left-hand side into an overdense plasma located on the right-hand side. $n_e/n_c=20$, $T_e=100\,\mathrm{eV}$, $T_e/T_i=3-5$, and the mass ratio $m_i/Zm_e=1836$. A Gaussian profile for the incident laser pulse was assumed in the simulation. Typically 150×2680 electrons and ions and 2680 cells were used. We consider an initial situation in which the ions are mobile and electrons are pulled out into vacuum by the component of electrical field normal to the target. The simulations show that an ''electron cloud'' always exists in front of the target, forming a strong negative electric field. This means a charge separation potential is generated and many hot electrons will be pushed back to the target surface.

The CSP we measured is greater than the prediction of

Bastiani *et al.* [20], calculated from the sheath-transit absorption (STA) of Yang *et al.* [11]. The sheath electric field is

$$E(x,t) = -\frac{m\nu_e^2}{e\lambda_D}\frac{2}{\sqrt{2}\exp(0.5)-(x/\lambda_D)} + \frac{2ck_y}{\omega} \times B_0\cos(\omega t+\phi). \quad (1)$$

The first term on the right-hand side of Eq. (1) is the sheath electrical field associated with the electrostatic potential to be determined by the self-consistent Poisson equation. If calculated with Eq. (1), the sheath potential under our experimental conditions is not more than 5 keV. That is much less than what we measured.

From our experimental conditions, we can calculate the CSP like this: the total electron number emitted from the target was measured to be about 6.5×10^9 for each shot [15]. The focal spot diameter was about 20 μm. The average distance between maximum positive and negative field is about 0.2λ (see Fig. 2), that is, 0.16 μm. Thus we can see that the electrons and less mobile ions form a ''capacitor'' of capacitance 7×10^{-15} F. So the potential on this ''capacitor'' is about 60 kV. This is more or less the same as we measured with the electron spectrometer.

The energy spectrum of hot electrons in Fig. 1 was measured at the same laser intensity with Al and glass targets. The peak position for the two target materials is almost the same but the maximum dose from Al targets is about four times that from glass targets, so there must be some effect decreasing the CSP in metallic targets relative to dielectric targets. One possible cause might be the great difference of electrical conductivity between metallic and dielectric targets. That is, when electrons are emitted from the focal spot of the target and generate the charge separation potential, this potential will be decreased immediately by free electrons in the metallic target, but the dielectric target has no free electrons to ''neutralize'' this potential due to its zero electrical conductivity.

This phenomenon can be observed also through measurement of the average hot electron energy and the total emitted electron number. The total number of escaping electrons from metallic targets can be measured exactly through the target potential [15] and is 6.5×10^9 at an intensity of 8×10^{15} W/cm^2. But the dielectric targets cannot be measured by this method. Other ways have to be found to solve this problem. A feasible way is to place a metallic probe (or metallic collector) in the direction normal to the target near the target surface. It can collect the emitted electrons. The first negative peak of the single diagram measured by the oscilloscope suggested that this was produced by escaping electrons. The value for the Al targets was about 1.6 V and 0.38 V for the glass targets. This showed that the total number of escaping electrons from Al targets is four times that from glass targets. The average energy of the emitted hot electrons was measured with a Faraday cup triggered by the target potential or the probe near the target surface. The distance from the focal spot to the Faraday cup was about 17 cm. In our experiment, the flight time from the target surface to the Faraday cup was about 1.5 ns for the Al target. This means the average hot electron energy was about 50 keV. The flight time was about 1.3 ns for glass targets. The average hot electron energy of glass is slightly greater than that of Al targets.

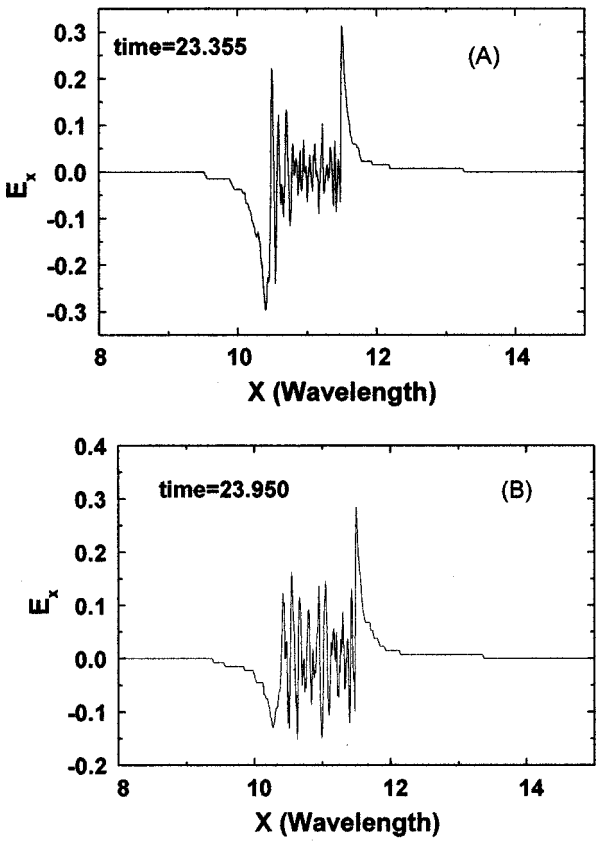

FIG. 3. The amplitude of the oscillating longitudinal electric field in glass targets at $t=23.355$ and 23.950 optical cycles. The solid surface is at $X=10.3$ (>10.3 is into the target).

According to the capacitor model, the CSP is proportional to the emitted electron number. But the CSP's we measured in Al and glass targets were almost the same. As the CSP builds up in Al targets at the focal spot, electrons around the focal spot are attracted to neutralize this potential instantly and cause decrease of the CSP. So, from Fig. 2, we cannot find a permanent positive electric field in the solid surface. But in dielectric targets (as shown in Fig. 3) the electrons near the focal spot are fixed. They cannot neutralize the less mobile ions, so this CSP keeps the same value.

Another difference between Al and glass targets associated with electrical conductivity is the laser absorption. With calorimeters, we measured the laser energy absorption in Al and glass targets shown in Fig. 4. The level of light scattered from the collecting optics was found to be negligible [7]. When the incident laser was focused on Al targets at 10^{13} W/cm^2, the reflection coefficient was about 80%, showing that the energy absorption for IB is near 20%. For the laser focused on Al targets at 8×10^{15} W/cm^2, the reflectivity dropped to 20%.

But this phenomenon did not occur for the glass targets. As the laser intensity increased, the reflection coefficient dropped to a minimum at the intensity of 10^{13} W/cm^2 and

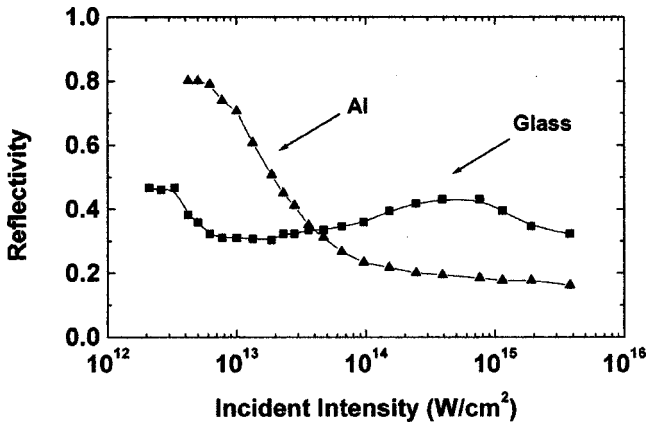

FIG. 4. The laser energy reflectivity vs laser intensity at 45° incidence on Al and glass targets.

then kept increasing up to 10^{15} W/cm^2. Compared with dielectric targets, metallic targets are easy to ionize and have many more electrons to form the plasma wave which contributes to the laser energy absorption. In other words, the laser can pump electrons from metallic targets continuously because of the metal's great electrical conductivity and those electrons can get more energy from the laser pulses. So the absorption coefficient in metallic targets is greater than that in dielectric targets. This process was shown clearly in Figs. 2 and 3. In metallic targets, the strong oscillating electric field will pull electrons out from inner target layers during the positive half period and push them out of the target surface in the negative half period. Electrons can be heated continuously in this way. But in dielectric targets a strong positive electric field is always exhibited behind the solid surface. This field reenforces the CSP and prevents electrons from accelerating. Of course, this phenomenon can also be explained numerically by the Fresnel equations in the Drude model, where the complex index of refraction $[n^2=1+i4\pi\sigma(\nu)/\omega]$ is related to the dc resistivity of the target material $(\rho_{\mathrm{dc}}=\nu m_e/N_e e^2)$.

IV. CONCLUSION

In summary, we have studied the energy absorption, hot electron emission, and hot electron energy spectrum produced during the interaction of a *p*-polarized laser pulse at 8×10^{15} W/cm^2 with metallic and dielectric target materials. The charge separation potential we measured was greater than the prediction of Yang *et al.* using the STA mechanism because the main heating process is the VH mechanism under our experimental conditions. In metallic targets the charge separation potential is lower than that of dielectric targets because free electrons continuously ''neutralize'' this potential. The laser absorption in metallic targets is higher than that in dielectric targets. The total number of electrons emitted from metallic targets is more than that from dielectric targets and the hot electron temperature in metallic targets is higher than that of dielectric targets.

ACKNOWLEDGMENTS

The authors would like to thank Professor Wei Yu for valuable discussions. This work was jointly supported by the National Natural Science Foundation of China under Grant Nos. 19825110 and 10075075 and the National Hi-Tech ICF Program.

[1] M. D. Perry and G. Mourou, Science **264**, 917 (1994).
[2] R. M. More *et al.*, J. Phys. (Paris), Colloq. **61**, C7-43 (1988).
[3] M. Tabak, J. Hammer, M. E. Glisky, W. L. Kruer, W. C. Wilks, and R. J. Mason, Phys. Plasmas **1**, 1626 (1994).
[4] A. Modena *et al.*, Nature (London) **377**, 606 (1995).
[5] P. A. Norreys, M. Zepf, S. Moustaizis, A. P. Fews, J. Zhang, P. Lee, M. Bakarezos, C. N. Danson, A. Dyson, P. Gibbon, P. Loukakos, D. Neely, F. N. Walsh, J. S. Wark, and A. E. Dangor, Phys. Rev. Lett. **76**, 1832 (1996).
[6] J. D. Kmetec, C. L. Gordon, J. J. Macklin, B. E. Lemoff, G. S. Brown, and S. E. Harris, Phys. Rev. Lett. **68**, 1527 (1992).
[7] D. F. Price, R. M. More, R. S. Walling, G. Guethlein, R. L. Shepherd, R. E. Stewart, and W. E. White, Phys. Rev. Lett. **75**, 252 (1995).
[8] A. Saemann and K. Eidmann, Appl. Phys. Lett. **73**, 1334 (1998).
[9] F. Brunel, Phys. Rev. Lett. **59**, 52 (1987); Phys. Fluids **31**, 2714 (1998).
[10] P. Gibbon and A. R. Bell, Phys. Rev. Lett. **68**, 1535 (1992); **73**, 664 (1994).
[11] P. J. Catto and R. M. More, Phys. Fluids **20**, 704 (1977); T.-Y. Brian Yang, William L. Kruer, Richard M. More, and A. Bruce Langdon, Phys. Plasmas **2**, 3146 (1995).
[12] T.-Y. Brian Yang, W. L. Kruer, A. B. Langdon, and T. W. Johnston, Phys. Plasmas **3**, 2702 (1996).
[13] P. Bilski *et al.*, Radiat. Prot. Dosim. **66**, 101 (1996).
[14] V. V. Ivanov, A. K. Knyazev, N. E. Korneev, A. A. Matsveiko, Yu. A. Mikhailov, V. P. Osetrov, A. I. Popov, G. V. Skizkov, and A. N. Starodub, Zh. Eksp. Teor. Fiz. **109**, 1257 (1996) [JETP **82**, 677 (1996)].
[15] L. Z. Zhao *et al.* (unpublished).
[16] P. Zhang, J. T. He, D. B. Chen, Z. H. Li, Y. Zhang, J. G. Bian, L. Wang, Z. L. Li, B. H. Feng, X. L. Zhang, D. X. Zhang, X. W. Tang, and J. Zhang, Phys. Rev. E **57**, 3746 (1997).
[17] W. L. Kruer, *The Physics of Laser Plasma Interactions* (Addison-Wesley, New York, 1988); S. J. Gitomen *et al.*, Phys. Fluids **29**, 2679 (1986); D. W. Forslund, J. M. Kindel, and K. Lee, Phys. Rev. Lett. **39**, 284 (1977).
[18] M. K. Grimes, A. R. Rundquist, Y. S. Lee, and M. C. Downer, Phys. Rev. Lett. **82**, 4010 (1999).
[19] L. M. Chen, J. Zhang, Q. L. Dong, H. Teng, T. J. Liang, L. Z. Zhao, and Z. Y. Wei (published).
[20] S. Bastiani, A. Rousse, J. P. Geindre, P. Audebert, C. Quoix, G. Hamoniaux, A. Antonetti, and J.-C. Gauthier, Phys. Rev. E **56**, 7179 (1997).